Translational Repression and eIF4A2 Activity Are Critical for MicroRNA-Mediated Gene Regulation

H. A. Meijer *et al.*

Science **340**, 82 (2013);
DOI: 10.1126/science.1231197

Translational Repression and eIF4A2 Activity Are Critical for MicroRNA-Mediated Gene Regulation

H. A. Meijer,* Y. W. Kong,* W. T. Lu,* A. Wilczynska,* R. V. Spriggs, S. W. Robinson, J. D. Godfrey, A. E. Willis, M. Bushell†

MicroRNAs (miRNAs) control gene expression through both translational repression and degradation of target messenger RNAs (mRNAs). However, the interplay between these processes and the precise molecular mechanisms involved remain unclear. Here, we show that translational inhibition is the primary event required for mRNA degradation. Translational inhibition depends on miRNAs impairing the function of the eIF4F initiation complex. We define the RNA helicase eIF4A2 as the key factor of eIF4F through which miRNAs function. We uncover a correlation between the presence of miRNA target sites in the 3′ untranslated region (3′UTR) of mRNAs and secondary structure in the 5′UTR and show that mRNAs with unstructured 5′UTRs are refractory to miRNA repression. These data support a linear model for miRNA-mediated gene regulation in which translational repression via eIF4A2 is required first, followed by mRNA destabilization.

MicroRNAs (miRNAs) are noncoding 21- to 25-nucleotide (nt) RNA molecules that in metazoans base-pair imperfectly with regions in target mRNAs [generally within the 3′ untranslated region (3′UTR)] and repress the synthesis of the corresponding proteins (*1*). The mechanism for miRNA-mediated repression has remained elusive. Nevertheless, it is clear that miRNAs bind target mRNAs in complex with Argonaute proteins (Ago1 to Ago4 in humans). This complex then recruits one of the trinucleotide repeat–containing proteins (TNRC6A to TNRC6C), and this in turn leads to both translational repression and mRNA destabilization (*1*).

To determine whether mRNA degradation is a cause or consequence of translational inhibition, we used transfection of in vitro transcribed let-7 target reporter mRNAs. Translational repression of the target mRNA can clearly be observed as early as 30 to 60 min after transfection in the absence of miRNA-dependent mRNA destabilization (fig. S1), which is in agreement with (*2*–*5*). As deadenylation occurs on miRNA-repressed mRNAs, we considered the requirement for the polyadenylate [poly(A)] tail in miRNA-mediated repression. Transfection of mRNAs with and without a poly(A) tail showed that unadenylated mRNAs are efficiently repressed by miRNAs, although the addition of a poly(A) tail increased the magnitude of repression (fig. S2, A and B). Although increasing the length of the poly(A) tail results in more efficient translation rates (fig. S2, C and D), we observed maximal repression of the let-7–targeted mRNA with a relatively short poly(A) tail (fig. S2E). Furthermore, we observed equally efficient repression of an mRNA with a poly(A) tail of exactly $(A)_{25}(C)_{10}$ as one with an $(A)_{25}$ tail, confirming that miRNA-mediated repression is not dependent on deadenylation (fig. S2, F and G). Both of these mRNAs can bind one poly(A)-binding protein (PABP) molecule (*6*); however, the former cannot be deadenylated (fig. S2, H and I) (*4*, *7*). Thus, the poly(A) tail, deadenylation, and mRNA degradation are not essential for miRNA-mediated translational repression, which is in agreement with other observations (*2*–*6*, *8*).

Evidence suggests that miRNAs exert their repressive activity at the translation initiation phase (*9*–*12*). To identify which translation initiation factors are required for repression, we appended the 5′UTRs of our reporter constructs with different internal ribosome entry site (IRES) sequences (Fig. 1A). The cricket paralysis virus (CrPV) IRES requires no initiation factors, binds directly to the ribosomal subunits, and promotes elongation (*1*). The hepatitis C virus (HCV) IRES binds directly to the 40*S* ribosomal subunit and only requires eIF3, eIF2, eIF5, eIF5B, and Met-$tRNA_i$, whereas the encephalomyocarditis virus (EMCV) IRES requires all initiation factors apart from eIF4E (*1*). A CrPV IRES mRNA containing let-7 target sites is not repressed, unlike the control mRNA (Fig. 1B), indicating that miRNA-mediated repression does not involve an elongation block, ribosome drop-off, or polypeptide degradation. The HCV IRES reporter was also refractory to miRNA-mediated repression, indicating that miRNA function is exerted before recruitment of the 60*S* ribosomal subunit, the eIF2-$tRNA_i$Met ternary complex, eIF3, eIF5, or eIF5B. In contrast, translation of a let-7 reporter driven by the EMCV IRES was repressed as efficiently as was cap-dependent translation, indicating that miRNA-mediated repression is exerted after eIF4E and eIF4G recruitment. The observed effects are not restricted to let-7 (fig. S3, A and B) and the IRESs are functional (fig. S3, C to F). Destabilization of the IRES-containing reporter mRNAs only occurred on translationally repressed messages (Fig. 1C), even though nonrepressed mRNAs remain associated with the targeting miRNAs (fig. S4, A to C) and the RNA-induced silencing complex (RISC) (fig. S4, D and E). Additionally, we confirmed that the CrPV IRES reporter mRNA can undergo destabilization (fig. S4F). Thus, translational repression is the primary and required event for miRNA-mediated control, followed by mRNA destabilization. A number of factors may explain previous contradictory results involving miRNA-targeted IRES reporters, including the presence of a poly(A) tail and method of mRNA delivery (*1*).

Our analysis of IRES-dependent miRNA-mediated repression excluded many of the translation initiation factors that might be implicated in the repression mechanism. The initiation factors that are required for EMCV IRES– but not

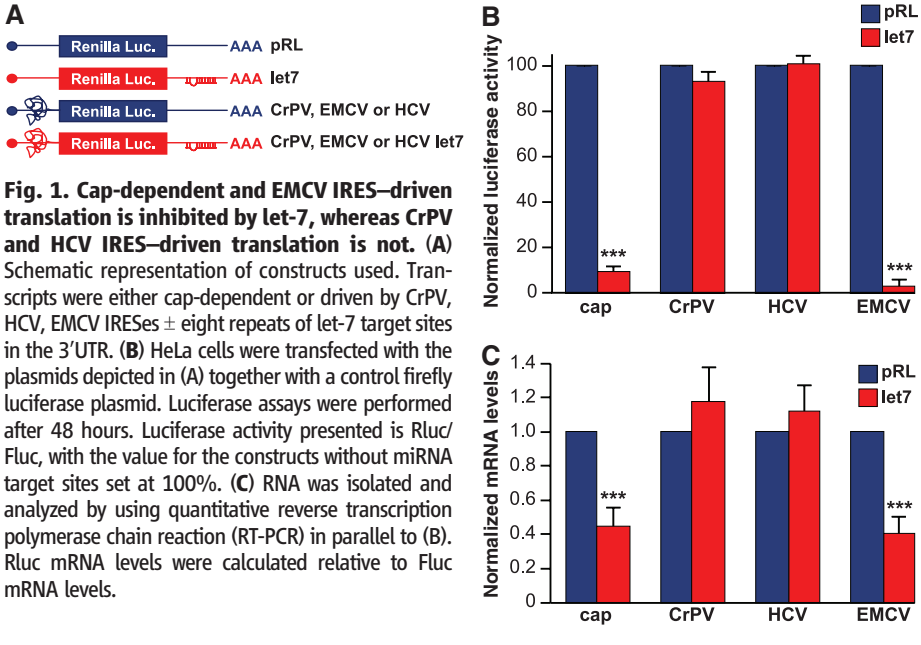

Fig. 1. Cap-dependent and EMCV IRES–driven translation is inhibited by let-7, whereas CrPV and HCV IRES–driven translation is not. (A) Schematic representation of constructs used. Transcripts were either cap-dependent or driven by CrPV, HCV, EMCV IRESes ± eight repeats of let-7 target sites in the 3′UTR. **(B)** HeLa cells were transfected with the plasmids depicted in (A) together with a control firefly luciferase plasmid. Luciferase assays were performed after 48 hours. Luciferase activity presented is Rluc/Fluc, with the value for the constructs without miRNA target sites set at 100%. **(C)** RNA was isolated and analyzed by using quantitative reverse transcription polymerase chain reaction (RT-PCR) in parallel to (B). Rluc mRNA levels were calculated relative to Fluc mRNA levels.

Medical Research Council (MRC) Toxicology Unit, Hodgkin Building, Lancaster Road, Leicester LE1 9HN, UK.

*These authors contributed equally to this work.
†Corresponding author. E-mail: mb446@le.ac.uk

HCV IRES–driven translation are all components of the eIF4F complex. To confirm that eIF4F function (which includes helicase activity and transcript scanning activity) is essential for repression, we transfected mRNAs carrying either the β-globin 5′UTR or an unstructured $(CAA)_{18}$ 5′UTR, which does not require unwinding (*13*), ± let-7 target sites (Fig. 2A). The mRNA bearing the unstructured 5′UTR was refractory to miRNA-mediated repression and even showed a slight activation (Fig. 2B), confirming a requirement for eIF4F, which is in agreement with (*11*, *12*).

To identify which of the implicated eIF4F components or associated factors are required for miRNA-mediated translational repression, small interfering RNAs (siRNAs) were used to knock down their expression, and DNA reporter constructs ± let-7 target sites were used as readout. Only the knockdown of eIF4A2 affected miRNA-mediated repression (Fig. 2, C to E). This effect was not specific to the particular eIF4A2 siRNA used or restricted to one cell type (fig. S5, A to E). Depletion of both eIF4As did not change the extent of derepression (fig. S5, F and G). siRNA-depletion of eIF4A2 also increased the expression of a number of well-known endogenous miRNA targets (Fig. 2E and fig. S5H) (*14*). The knockdown of eIF4A2 or TNRC6A+B, but not eIF4A1, resulted in stabilization of reporter mRNA with let-7 target sites (Fig. 2F), again showing the requirement for translational repression for mRNA destabilization. Together, these results identify the eIF4F component eIF4A2 as the primary and key factor for miRNA-mediated gene silencing. To examine the early events in the miRNA repression pathway, before mRNA destabilization, the expression of either eIF4A2 or TNRC6A+B was knocked down, followed by transfection of in vitro transcribed mRNAs ± let-7 target sites for 1 hour. At this time point, siRNA depletion of eIF4A2 or TNRC6A+B had similar effects on the miRNA target (Fig. 2, G and H, and fig. S5I). Transfection of a dominant negative form of eIF4A1 inhibited translation but did not affect the extent of miRNA-mediated regulation (fig. S6, A to C), whereas inhibition of both eIF4As with Pateamine A lead to a marked decrease in miRNA-mediated repression (fig. S6, D and E). Rescue experiments showed that after depletion of eIF4A2, only eIF4A2 and not eIF4A1 can restore repression (Fig. 2, I and J, and fig. S6, F and G),

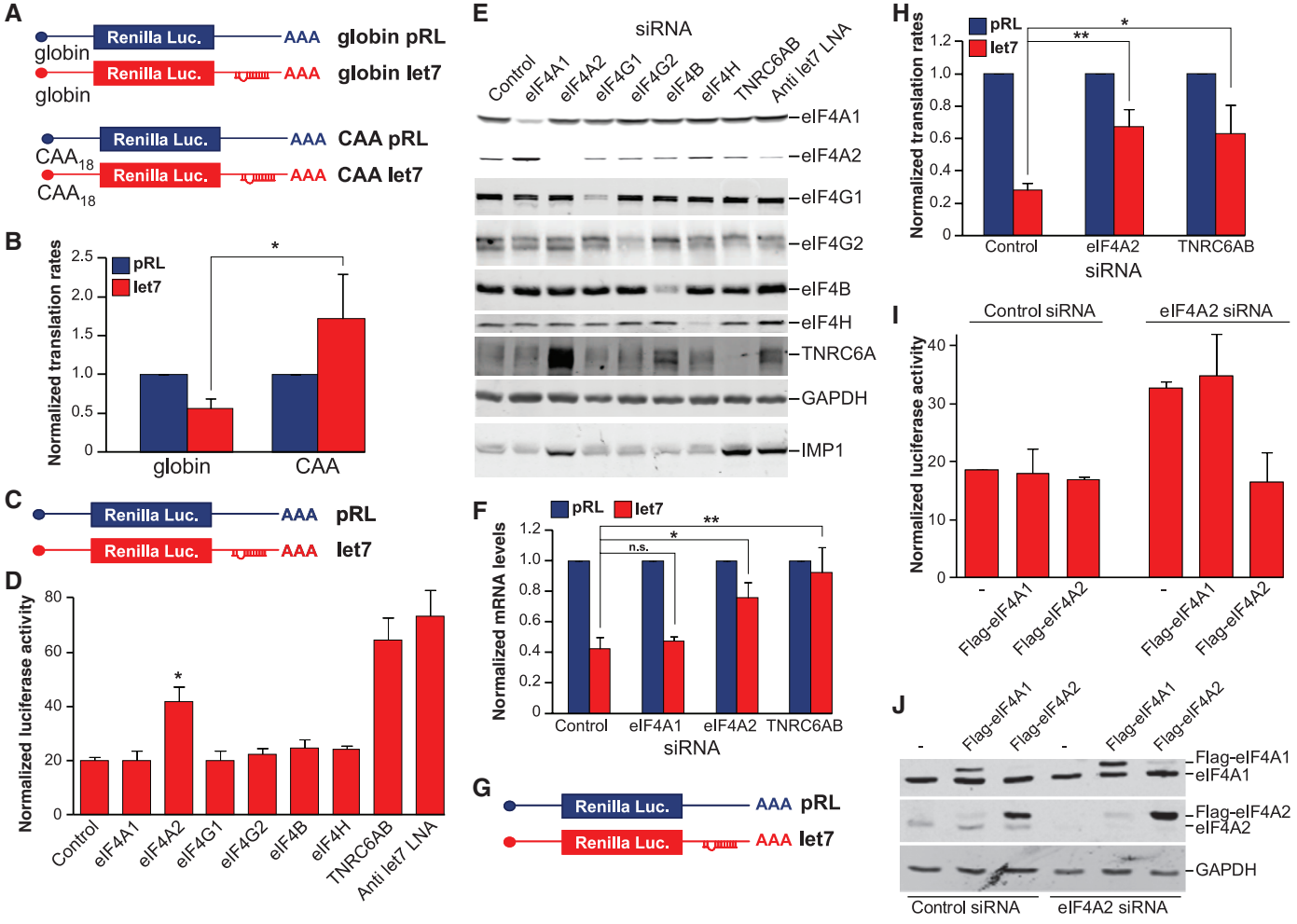

Fig. 2. eIF4A2 is the only component of eIF4F required for miRNA-mediated repression. (**A**) Schematic representation of transcripts used for transfection with either the β-globin 5′UTR or an unstructured $(CAA)_{18}$ 5′UTR ± two let-7 target sites. (**B**) HeLa cells were transfected with the in vitro transcribed mRNAs depicted in (A). Protein and RNA were harvested after 90 min. Translation rates were determined as a ratio of luciferase activity to mRNA levels (four biological repeats). (**C**) Constructs used for transfection in (D) to (F), ± two let-7 target sites. (**D**) HeLa cells were transfected with the indicated siRNAs or an LNA against let-7 for 48 hours. Next, cells were transfected with the plasmid constructs depicted in (C) and the Firefly luciferase control. Luciferase activity was assayed after 24 hours. Values for control reporters were set at 100%. (**E**) HeLa cells were transfected in parallel with (D). Lysates were analyzed by means of Western blot as indicated. IMP1 is a target of let-7. (**F**) HeLa cells were transfected as in (D), RNA isolated and analyzed by means of quantitative RT-PCR. Rluc mRNA levels were calculated relative to Fluc mRNA. (**G**) Transcripts used for transfection, ± eight let-7 target sites. (**H**) HeLa cells were transfected with the indicated siRNAs. After 3 days, the cells were trypsinised, counted, and transfected with the in vitro transcribed mRNA depicted in (G). RNA and protein was collected after 60 min, and the translation rates were calculated (four biological repeats). (**I**) HeLa cells were transfected with the indicated siRNAs. Plasmids encoding the indicated Flag-tagged proteins were transfected after 24 hours, and reporters as depicted in (C) after another 24 hours. Luciferase assays were performed after a further 24 hours as in (D). (**J**) HeLa cells were transfected in parallel with (I). Lysates were analyzed by means of Western blot as indicated.

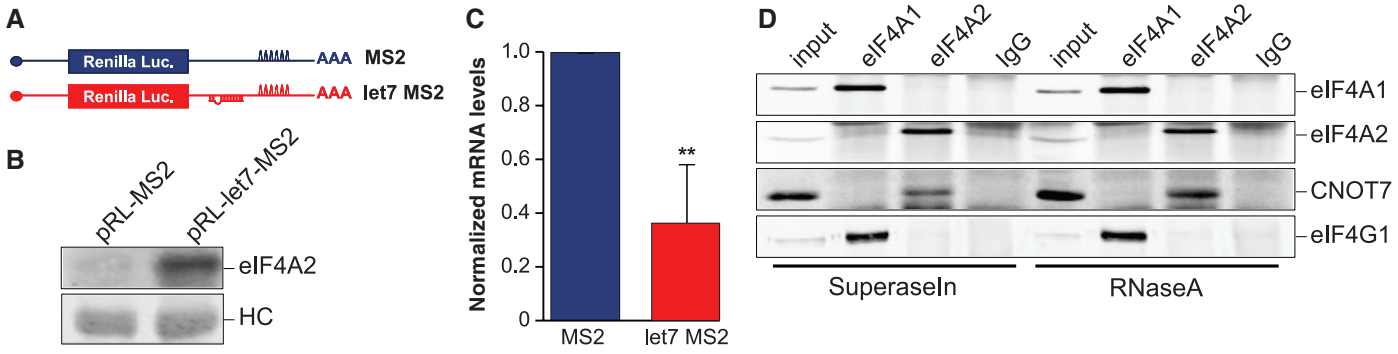

Fig. 3. eIF4A2 is preferentially recruited to miRNA-targeted mRNAs and specifically associates with CNOT7, a component of the miRNA-repression machinery. (**A**) Schematic representation of tethering constructs with 12 repeats of the MS2 hairpin within the 3′UTR ± eight let-7 target sites. (**B**) MS2 immunoprecipitation of let-7–repressed mRNAs shows greater association with eIF4A2. HeLa cells were transfected with the plasmid constructs depicted in (A) together with a plasmid-expressing Flag-tagged MS2 coat protein. After 48 hours, cells were lysed and subjected to Flag immunoprecipitation followed by Western blot analysis. HC, heavy chain. (**C**) Experiment as in Fig. 3B, analyzed by means of quantitative RT-PCR. (**D**) Immunoprecipitation from untransfected HeLa cell lysates using specific antibodies to eIF4A1 and eIF4A2 with ribonuclease (RNAse) A or with RNase inhibitor (SuperaseIn). Recovered proteins were analyzed by using Western blot. Input, 10%.

confirming that eIF4A2 plays a critical role early in the repression pathway independently of eIF4A1.

eIF4A1 and eIF4A2 are both adenosine 5′-triphosphate (ATP)–dependent RNA helicases, believed to be involved in unwinding secondary structure within the 5′UTR of mRNAs, thus allowing the 40*S* ribosomal subunit to dock and scan toward the start codon (*1*). These highly related factors share 90% similarity at the protein level, with the major differences residing within the N-terminal domain. Although eIF4A1 is generally in excess of eIF4A2, they do not have identical functions (*15*). This prompted us to explore the possibility that eIF4A2, but not eIF4A1, was specifically interacting with microribonucleoprotein complexes. To determine whether endogenous eIF4A2 associated with miRNA-repressed mRNAs, MS2 binding protein was used to immunopurify mRNAs containing MS2 hairpins ± let-7 target sites within their 3′UTR. Western blotting was used to identify associated proteins. This experiment clearly shows that eIF4A2 specifically associates with let-7–repressed mRNAs (Fig. 3, A to C). Members of the TNRC6 protein family have been shown to interact with the Ccr4-NOT complex to induce both translational repression and mRNA deadenylation (*16*–*19*). Because a recent structural study has shown that cNOT1, a central component of this complex, contains a MIF4G fold similar to the eIF4A binding site of eIF4G (*20*), we investigated whether eIF4A2 interacts with the Ccr4-NOT complex. Indeed, immunoprecipitation of endogenous eIF4A2, but not of eIF4A1, reveals a specific RNA-independent association of eIF4A2 with CNOT7 (Fig. 3D). We also observed that eIF4G is preferentially associated with eIF4A1 (Fig. 3D), which was independently confirmed (fig. S6H).

Our results imply that mRNAs with functional miRNA-target sites in their 3′UTR would require structured 5′UTRs to enable repression. To examine this globally, 5′UTR structure prediction was performed by using RNAfold on the human RefSeq database. The mRNAs were grouped depending on the presence or absence of conserved miRNA target sites in their 3′UTR as predicted with TargetScan (Fig. 4). mRNAs with miRNA target sites are more likely to have a greater degree of secondary structure within their 5′UTR. We reasoned that mRNAs with short 5′UTRs (less than 100 nt) should be even more dependent on secondary structure for miRNA-mediated activity. Indeed, we observed a stronger relationship between structure and the presence of conserved miRNA target sites within short 5′UTRs (Fig. 4).

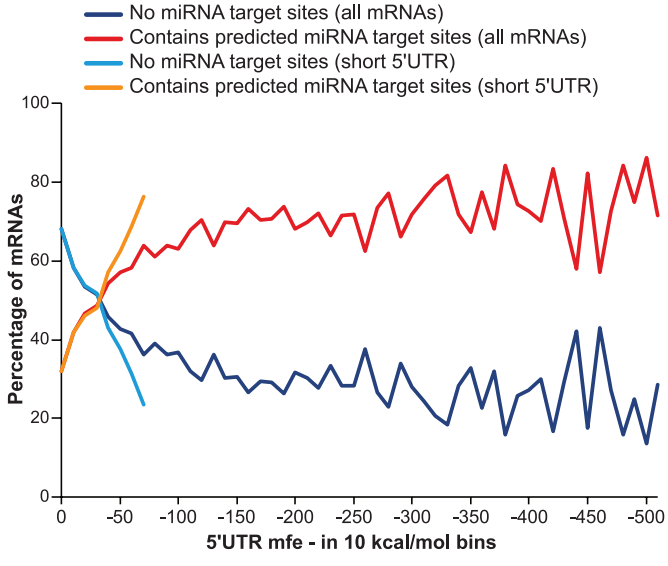

Fig. 4. mRNAs with miRNA target sites in their 3′UTR have a greater degree of secondary structure in the 5′UTR than do mRNAs without miRNA target sites. 5′UTR sequences were analyzed by using RNAfold for potential secondary structure and grouped into 10 kcal/mol-wide minimum free-energy (mfe) bins. mRNAs within each bin were interrogated for conserved miRNA target sites. mRNAs with relatively short 5′UTRs (between 18 and 100 nt) were analyzed separately. Statistical significance for all mRNAs, $P = 1.84 \times 10^{-197}$; for short 5′UTR mRNAs, $P = 1.06 \times 10^{-22}$.

Our data show that miRNAs induce gene silencing with translational repression occurring first and being required for subsequent mRNA destabilization. Moreover, we demonstrate that eIF4A2 and structure within the 5′UTR of target mRNAs are critical for miRNA-mediated repression. We show that eIF4A2 interacts with components of the repression machinery, namely the Ccr4-NOT complex. Interaction may be occurring via the MIF4G domain within cNOT1 (*20*) recruiting eIF4A2 and imposing translational repression. The presence of eIF4A2 on a repressed mRNA via its interaction with the Ccr4-NOT complex would preclude the progression of initiation directed by eIF4G and eIF4A1, both for EMCV IRES– and, more importantly, cap-dependent translation.

References and Notes

1. R. J. Jackson, C. U. Hellen, T. V. Pestova, *Nat. Rev. Mol. Cell Biol.* **11**, 113 (2010).
2. M. R. Fabian *et al.*, *Mol. Cell* **35**, 868 (2009).
3. S. Djuranovic, A. Nahvi, R. Green, *Science* **336**, 237 (2012).
4. A. A. Bazzini, M. T. Lee, A. J. Giraldez, *Science* **336**, 233 (2012).
5. J. Béthune, C. G. Artus-Revel, W. Filipowicz, *EMBO Rep.* **13**, 716 (2012).
6. F. Moretti, C. Kaiser, A. Zdanowicz-Specht, M. W. Hentze, *Nat. Struct. Mol. Biol.* **19**, 603 (2012).
7. Y. Mishima *et al.*, *Proc. Natl. Acad. Sci. U.S.A.* **109**, 1104 (2012).
8. L. Wu, J. Fan, J. G. Belasco, *Proc. Natl. Acad. Sci. U.S.A.* **103**, 4034 (2006).
9. R. S. Pillai *et al.*, *Science* **309**, 1573 (2005).
10. R. Thermann, M. W. Hentze, *Nature* **447**, 875 (2007).
11. G. Mathonnet *et al.*, *Science* **317**, 1764 (2007).

12. A. Zdanowicz *et al.*, *Mol. Cell* **35**, 881 (2009).
13. T. V. Pestova, V. G. Kolupaeva, *Genes Dev.* **16**, 2906 (2002).
14. B. Boyerinas *et al.*, *Cancer Res.* **68**, 2587 (2008).
15. G. Galicia-Vázquez, R. Cencic, F. Robert, A. Q. Agenor, J. Pelletier, *RNA* **18**, 1373 (2012).
16. M. Chekulaeva *et al.*, *Nat. Struct. Mol. Biol.* **18**, 1218 (2011).
17. J. E. Braun, E. Huntzinger, M. Fauser, E. Izaurralde, *Mol. Cell* **44**, 120 (2011).
18. M. R. Fabian *et al.*, *Nat. Struct. Mol. Biol.* **18**, 1211 (2011).
19. A. Cooke, A. Prigge, M. Wickens, *J. Biol. Chem.* **285**, 28506 (2010).
20. A. P. Petit *et al.*, *Nucleic Acids Res.* **40**, 11058 (2012).

Acknowledgments: We thank E. Smith, M. Stoneley, T. Pöyry, E. Jan, C. Jopling, T. Achsel, M. Hentze, and J. Pelletier for helpful comments and reagents. This work was funded by the MRC, UK. M.B. is an MRC Senior Fellow, and A.E.W. is a Biotechnology and Biological Sciences Research Council Professorial Fellow.

Supplementary Materials
www.sciencemag.org/cgi/content/full/340/6128/82/DC1
Materials and Methods
Supplementary Text
Figs. S1 to S6
References (*21*–*38*)

8 October 2012; accepted 31 January 2013
10.1126/science.1231197

Archaeal (Per)Chlorate Reduction at High Temperature: An Interplay of Biotic and Abiotic Reactions

Martin G. Liebensteiner,[1] Martijn W. H. Pinkse,[2,3] Peter J. Schaap,[4] Alfons J. M. Stams,[1,5]* Bart P. Lomans[6]

Perchlorate and chlorate anions [(per)chlorate] exist in the environment from natural and anthropogenic sources, where they can serve as electron acceptors for bacteria. We performed growth experiments combined with genomic and proteomic analyses of the hyperthermophile *Archaeoglobus fulgidus* that show (per)chlorate reduction also extends into the archaeal domain of life. The (per)chlorate reduction pathway in *A. fulgidus* relies on molybdo-enzymes that have similarity with bacterial enzymes; however, chlorite is not enzymatically split into chloride and oxygen. Evidence suggests that it is eliminated by an interplay of abiotic and biotic redox reactions involving sulfur compounds. Biological (per)chlorate reduction by ancient archaea at high temperature may have prevented accumulation of perchlorate in early terrestrial environments and consequently given rise to oxidizing conditions on Earth before the rise of oxygenic photosynthesis.

Perchlorate and chlorate anions [together referred to as (per)chlorate] in the environment have long been considered as arising mainly from anthropogenic activities, namely the production of perchlorate-containing rocket propellants and ammunitions followed by environmental pollution (*1*). However, recent findings indicate that perchlorate is continuously formed naturally in the atmosphere, with proposed mechanisms ranging from photochemically triggered processes (*2*) to electrical discharge–based reactions and ozone oxidation of chlorides (*3*). Such natural sources make perchlorate an ubiquitous compound on Earth, although sizeable accumulations tend to be limited to certain arid environments, like the Atacama desert in Chile (*4*). Perchlorate deposits also exist on Mars (*5*). It has been proposed that the lack of perchlorate accumulation elsewhere on Earth might be due to microbial activity (*4*), which is supported by the widespread occurrence of bacteria that can use perchlorate and chlorate as terminal electron acceptor for growth (*6*).

(Per)chlorate-reducing bacteria described so far belong mainly to the bacterial phylum of Proteobacteria (*7*). The widely accepted pathway of biological (per)chlorate reduction consists of a two-step reduction from perchlorate, via chlorate to chlorite, followed by a dismutation to molecular oxygen and chloride (*8*). This metabolism relies on the action of a perchlorate reductase (Pcr) and a chlorate reductase (Clr), two functions that in perchlorate reducers are often performed by a single enzyme (*9*); it further requires a chlorite dismutase (Cld) to form molecular oxygen and chloride. Microbial formation of molecular oxygen under anaerobicity is a biochemical rarity.

Because the reported mechanisms for natural perchlorate generation on Earth seem to have existed already during preanthropogenic times (*1*, *2*), the appearance of biological reduction of (per)chlorate may have been an important event in Earth's history. One indication of an ancient origin for reduction of (per)chlorate would be its occurrence in microorganisms that thrive in environments resembling those of early Earth. *Archaeoglobus fulgidus*, a hyperthermophilic archaeon, fulfills this criterion. *A. fulgidus* was isolated from marine hot vents close to Vulcano island in Italy (*10*) but has since then been found in many extreme subsurface environments, such as hot oil reservoirs or geothermal formations (*11*, *12*). It is considered to be a major contributor to sulfate reduction and sulfide formation at high temperature. *A. fulgidus* strain VC-16 is the best-studied sulfate-reducing archaeon. Its genome contains many oxidoreductases genes with unknown function (*13*).

We demonstrate that *A. fulgidus* strain VC-16 as well as *A. fulgidus* strain Z (*14*) (fig. S1) can grow with perchlorate or chlorate as electron acceptors (Fig. 1 and table S1). Our finding extends (per)chlorate reduction into the archaeal domain of life and high temperature environments.

Enzyme assays showed chlorate-reducing activity in cell-free extracts and suspensions of *A. fulgidus* VC-16 that were comparable with activities found in some mesophilic (per)chlorate-reducing bacteria (table S2). An activity toward perchlorate could not clearly be identified, which is similar to an earlier study on the (per)chlorate reductase of *Azospira oryzae* strain GR-1 (*9*). No chlorite dismutase activity could be detected, either. Consistent with this, no genes similar to known chlorite dismutases were identified in the genome of *A. fulgidus*. On the other hand, no accumulation of chlorite was observed, suggesting an alternative mechanism of chlorite conversion.

Perchlorate- and chlorate-grown cells of *A. fulgidus* are still able to use sulfate as electron acceptor. When sulfate and perchlorate are present together in the cultures, both are used simultaneously, whereas sulfate reduction is delayed if chlorate is present (Fig. 1, C and D). Simultaneous perchlorate and sulfate reduction in a single culture is intriguing from an energetic viewpoint. The midpoint potentials of redox couples involved in (per)chlorate reduction are high, whereas those involved in sulfate reduction are low [for ClO_4^-/ClO_3^-, redox potential ($E^{0\prime}$) = +0.788 V; ClO_3^-/ClO_2^- $E^{0\prime}$ = +0.709 V; ClO_2^-/Cl^- $E^{0\prime}$ = +1.199 V versus SO_4^{2-}/HSO_3^- $E^{0\prime}$ = –0.516 V; HSO_3^-/HS^- $E^{0\prime}$ = –0.110 V]. During the reduction of (per)chlorate, the redox potential is locally increasing, but the overall redox state remains low in all the cultures throughout the entire experiment (≤ –200 mV), indicated by resazurin in the medium and a redox electrode.

Sulfide is normally omitted from media when growing (per)chlorate reducers but is used to establish the low redox potential required for growth of strict anaerobes like *A. fulgidus*. Similar to sulfate reduction, (per)chlorate reduction in *A. fulgidus* requires reduced conditions that are established by the addition of sulfide to the medium and even pronounced by sulfide formation if sulfate is present as well (Fig. 1, C and D).

Proteome analysis of cells grown with either perchlorate or chlorate shows that, in comparison with sulfate-grown cells, there is an increased abundance of a large number of proteins that are associated with redox and oxygen stress (table S3). We hypothesize that in the presence of (per)chlorate these proteins play a crucial role in creating and maintaining a low intracellular redox potential, which is a basic requirement for dissimilatory sulfate reduction. The differential expression of

[1]Laboratory of Microbiology, Wageningen University, Dreijenplein 10, 6703 HB Wageningen, Netherlands. [2]Analytical Biotechnology Section, Department of Biotechnology, Delft University of Technology, Julianalaan 67, 2628 BC Delft, Netherlands. [3]Netherlands Proteomics Centre, Julianalaan 67, 2628 BC Delft, Netherlands. [4]Laboratory of Systems and Synthetic Biology, Wageningen University, Dreijenplein 10, 6703 HB Wageningen, Netherlands. [5]Centre of Biological Engineering, University of Minho, Campus de Gualtar, 4710-057 Braga, Portugal. [6]Shell Global Solutions International B.V., Kessler Park 1, 2288 GS Rijswijk, Netherlands.

*Corresponding author. E-mail: Fons.Stams@wur.nl